

# Effect of nitrite and nitrate on biogenic sulfide production in sewer biofilms determined by the use of microelectrodes

S. Okabe\*, T. Ito\*, H. Satoh\*\* and Y. Watanabe\*\*

\* Department of Urban and Environmental Engineering, Graduate School of Engineering, Hokkaido University, North-13, West-8, Sapporo 060-8628, Japan (E-mail: [sokabe@eng.hokudai.ac.jp](mailto:sokabe@eng.hokudai.ac.jp))

\*\* Department of Civil Engineering, Hachinohe Institute of Technology, Hachinohe, Aomori 031-8501, Japan

**Abstract** The effects of  $O_2$  and  $NO_3^-$  concentrations on *in situ* sulfate reduction and sulfide reoxidation in microaerophilic wastewater biofilms grown on rotating disk reactors were investigated by the use of microelectrodes for  $O_2$ ,  $S^{2-}$ ,  $NO_3^-$ ,  $NO_2^-$ , and pH. Microelectrode measurements showed the vertical microzonation of  $O_2$  respiration,  $NO_3^-$  respiration,  $H_2S$  oxidation and  $SO_4^{2-}$  reduction in the biofilms. The microelectrode measurements indicate that sulfate reducing activity was largely restricted to a narrow anaerobic zone located about 500  $\mu m$  below the biofilm surface. An addition of nitrate forced the sulfate reduction zone deeper in the biofilm and reduced the specific sulfate reduction rate as well. The sulfate reduction zone was consequently separated from the  $O_2$  and  $NO_3^-$  respiration zones. Anaerobic  $H_2S$  oxidation with  $NO_3^-$  was also induced by addition of nitrate to the medium. Measurements of the reduced inorganic sulfur compounds ( $FeS$ ,  $FeS_2$  and  $S^0$ ), total-Mn and total-Fe in the biofilm indicated that the produced  $H_2S$  became immediately oxidized with  $O_2$ ,  $NO_3^-$  and other oxidants, mainly ferric/ferrous hydrates. On the basis of the present results, it was estimated that of all sulfide produced, 13% of the sulfide was precipitated by metal ions as  $FeS$  and  $S^0$  just above the sulfate reduction zone, 65% was anaerobically oxidized to  $SO_4^{2-}$  with  $NO_3^-$  as an electron acceptor and 22% was aerobically oxidized within the biofilm incubated in 70  $\mu mol\ l^{-1}$  of DO and 280  $\mu mol\ l^{-1}$  of  $NO_3^-$ .

**Keywords** Microelectrodes; nitrate; sewer biofilms; sulfate reduction

## Introduction

Although sulfate reduction accounts for up to 50% of the mineralization of organic matter in aerobic wastewater treatment systems (Kühl and Jorgensen, 1992), sulfate-reducing bacteria (SRB) cause serious problems in sanitary sewer systems and industrial water systems because of production of highly toxic and corrosive hydrogen sulfide ( $H_2S$ ) gas. Furthermore, once sulfate reduction occurs in biofilms, internal sulfide reoxidation is expected to account for a substantial part of oxygen consumption (approximately up to 70%) (Kühl and Jorgensen, 1992; Norsker *et al.*, 1995; Santegoeds *et al.*, 1998). A major drawback of  $H_2S$  production in wastewater treatment systems is that  $H_2S$  is a precursor of odorants and significantly enhances microbially mediated corrosion of sewer pipes and treatment facilities (Hamilton, 1985; Mori *et al.*, 1992; Postgate, 1984). Even though the bulk wastewater is oxygenated, sulfate reduction occurs in the deeper anaerobic biofilm attached on the concrete surface (Okabe *et al.*, 1999; Ramsing *et al.*, 1993; Santegoeds *et al.*, 1998). Such toxicity and corrosive properties of  $H_2S$  dictate stringent control of the  $H_2S$  production in sewer systems. Inhibiting the growth of SRB can directly or indirectly prevent sulfide production by SRB. Aeration and biocides are common approaches. However, since SRB are generally found in biofilms, in which oxygen and biocides do not effectively penetrate through the biofilm, these measures are of limited effectiveness.

Therefore, in this study, nitrate and nitrite were added to sewer biofilm systems to effectively control biogenic sulfide production. To evaluate the efficacy of nitrite and nitrate

addition and to understand details of inhibition mechanisms of sulfide production in biofilms, we applied microelectrodes to measure fine-scale *in situ* sulfide production activity in the biofilm. Because mass balance of sulfide or sulfate flux across a biofilm-liquid interface cannot describe sulfur transformations within the biofilm due to the presence of a complex internal sulfur cycle in oxic/anoxic sewer biofilms. We will present the effect of oxygen, nitrate, and nitrite concentrations on the *in situ* sulfide production activity within biofilms by using microelectrodes.

## Experimental materials and methods

### Biofilm samples

Microaerophilic mixed population biofilms were grown in rotating disk reactors (RDR) consisting of 5 poly-methyl-methacrylate disks. Eight removable slides ( $1 \times 6$  cm) were installed in each disk for sampling biofilms. The reactor volume was  $1,370 \text{ cm}^3$  and total biofilm area was  $2,830 \text{ cm}^2$ . Disk rotational speed was fixed at 14 rpm. Dilution rate in the reactors was kept at  $0.2 \text{ h}^{-1}$ . The primary settling tank effluent from the municipal wastewater treatment plant (consisting of stage 1 (215,000 PE) and 2 (210,000 PE), population equivalents [PE], 1PE = 60 g of biological oxygen demand per day) at Sapporo, Japan was fed into the reactor. Average dissolved oxygen concentration in the bulk liquid was  $40 \pm 30 \mu\text{mol l}^{-1}$  during the experiment. After effluent water quality reached the steady state, the biofilm samples were taken for microelectrode measurements.

### Microelectrode measurements

Concentration gradients of  $\text{O}_2$ ,  $\text{NO}_2^-$ ,  $\text{NO}_3^-$ , pH, and  $\text{S}^{2-}$  in the biofilms were measured by microelectrodes manufactured in our laboratory. Cathode type oxygen microelectrodes with a tip diameter of about  $15 \mu\text{m}$  were prepared and calibrated as described previously by Revsbech (1989). Liquid ion-exchanging membrane (LIX) microsensors with tip diameters of about  $10\text{--}15 \mu\text{m}$  for  $\text{NH}_4^+$ ,  $\text{NO}_2^-$ ,  $\text{NO}_3^-$ , and pH were prepared according to deBeer *et al.* (1997). Lix microsensors were calibrated in dilution series ( $10^{-3}\text{--}10^{-6} \text{ mol l}^{-1}$ ) of  $\text{NH}_4^+$ ,  $\text{NO}_2^-$ , and  $\text{NO}_3^-$  in the medium used for the measurements. The pH microelectrode was calibrated in the culture medium adjusted for pH in the range 4 to 9. The sulfide electrodes were manufactured as described by Revsbech and Jorgensen (1986) and calibrated as described by Kuhl and Jorgensen (1992). Total sulfide concentration ( $\text{H}_2\text{S}$ ,  $\text{HS}^-$  and  $\text{S}^{2-}$ ) in the dilution series was determined by the methylene blue method (Cline, 1969). The measuring circuit was the same as for pH measurements. The 90% response times were approximately 1 to 30 min, depending on sulfide concentration. Since the pH profiles showed a significant variation ( $>0.1$  pH unit) through the biofilm, pH correction of the measured sulfide profiles was necessary. The total sulfide concentration ( $\text{S}_\text{T}$ ) in an aqueous solution can be calculated as described by Kuhl and Jorgensen (1992). We used the following dissociation constants for sulfide,  $\text{pK}_1 = 7.05$  and  $\text{pK}_2 = 17.1$  (Millero and Hershey, 1989).

### Microelectrode measurements

Biofilms were taken from the reactors and incubated in the synthetic medium and in the dark for about 3 hours before measurements were made, which ensured steady-state concentration profiles. The medium contained the following ( $\mu\text{mol l}^{-1}$ ):  $\text{NaNO}_3$  (270);  $\text{NaNO}_2$  (100);  $\text{MgSO}_4 \cdot 7\text{H}_2\text{O}$  (1000); sodium propionate (600);  $\text{NH}_4\text{Cl}$  (300);  $\text{Na}_2\text{HPO}_4$  (570);  $\text{MgCl}_2 \cdot 6\text{H}_2\text{O}$  (84);  $\text{CaCl}_2$  (200);  $\text{EDTA} \cdot 2\text{Na}$  (270). All measurements were performed in the dark and in a water chamber containing 1.8 litre of the synthetic medium at  $20^\circ$ . Each microelectrode was separately mounted on a motor-driven micromanipulator (Chuo seiki, ACV-104-HP, Japan). The electrode assembly was placed inside a Faraday cage to reduce

electrical noise. Each measurement was performed three to five times by advancing the electrodes at depth steps of 50 to 100  $\mu\text{m}$  through the biofilm. Average liquid flow velocity (2–3  $\text{cm s}^{-1}$ ) above the biofilm was provided by a Pasteur pipette blowing a mixture of air and  $\text{N}_2$  gas onto the water surface. The bulk  $\text{O}_2$  concentration was kept the same as that in the RDR, i.e. ca. 70  $\mu\text{mol l}^{-1}$ . The biofilm-liquid interface was determined by using a dissection microscope (Stemi 2000, Carl Zeiss).

#### Estimations of specific reaction rates and substrate flux

Net specific consumption and production rates were estimated from the measured micro-profiles by using the Fick's second law of diffusion. The detail of this method has been previously described by Lorenzen *et al.* (1998). Furthermore, the dimensional diffusion fluxes ( $J$ ) through the biofilm-liquid interface were calculated by using Fick's first law:  $J = -D_s$  ( $dS/dz$ ), where  $D_s$  is the molecular diffusion coefficient of compound  $S$  in the liquid phase,  $dS/dz$  is the concentration gradient in the boundary layer at the biofilm-liquid interface. We used the molecular diffusion coefficients of  $2.09 \times 10^{-5} \text{ cm}^2 \text{ s}^{-1}$  for oxygen,  $1.23 \times 10^{-5} \text{ cm}^2 \text{ s}^{-1}$  for  $\text{NO}_3^-$  (Andrussow, 1969), and  $1.39 \times 10^{-5} \text{ cm}^2/\text{s}$  for total sulfide (Kühl and Jorgensen, 1992), respectively at 20°.

#### Measurement of reduced sulfur compounds

Elemental sulfur ( $\text{S}^0$ ), acid-volatile sulfides (AVS;  $\text{H}_2\text{S}$  and  $\text{FeS}$ ) and chromium reducible sulfide (CRS;  $\text{FeS}_2$ ) in biofilms were determined by the method described originally by Fossing and Jorgensen (1989) and modified by Nielsen *et al.* (1993). The biofilm samples were immediately fixed in 1% zinc acetate solution and were sequentially analyzed for elemental sulfur ( $\text{S}^0$ ), AVS ( $\text{H}_2\text{S}$  and  $\text{FeS}$ ) and CRS ( $\text{FeS}_2$ ). Elemental sulfur was extracted by 96% ethanol for 24 h at room temperature *prior to* AVS and CRS measurements. Samples extracted in ethanol were analyzed by a HPLC with a UV detector at 254 nm. A reversed phase column (Partisil 5, ODS-3 Whatman) was used with 100% HPLC grade methanol (138-06473, Wako) as eluent and flow rate of 0.4 ml/min. The sample injection volume was 100  $\mu\text{l}$ . The remaining samples from ethanol extraction were resuspended in 10 ml of 1% ZnAC solution and AVS ( $\text{H}_2\text{S}$  and  $\text{FeS}$ ) was volatilized by addition of 10 ml of 2 mol  $\text{l}^{-1}$  HCl. The volatilized  $\text{H}_2\text{S}$  was trapped in 1% ZnAC solution (variable volumes) and measured colorimetrically by the methylene blue method. After the AVS distillation, 2.5 mL of 1 mol  $\text{l}^{-1}$   $\text{Cr}^{2+}$  in 0.5 mol  $\text{l}^{-1}$  HCl solutions was added directly to the remaining sample suspension from  $\text{S}^0$  and AVS analyses. CRS was volatilized and  $\text{H}_2\text{S}$  was measured as described above. Recovery of  $\text{FeS}$  and  $\text{FeS}_2$  was determined previously to be  $87 \pm 7\%$  ( $n = 3$ ) and  $73 \pm 24\%$  ( $n = 3$ ), respectively.

## Results and discussion

### Effect of $\text{O}_2$ and $\text{NO}_3^-$ on sulfate reduction

Typical concentration profiles of  $\text{O}_2$ ,  $\text{H}_2\text{S}$ , T-S and pH in a biofilm incubated in  $\text{DO} = 156 \mu\text{mol l}^{-1}$  and  $\text{NO}_3^- = 0 \mu\text{mol l}^{-1}$  are shown in Figure 1. Oxygen penetrated only about 500  $\mu\text{m}$  from the surface in a 1,500  $\mu\text{m}$ -thick biofilm. At even this bulk DO level, sulfide was produced 700–1,000  $\mu\text{m}$  below the surface at a specific rate of 16.4  $\text{H}_2\text{S} \mu\text{mol cm}^{-3} \text{ h}^{-1}$ . Below the sulfate reduction zone, the constant  $\text{H}_2\text{S}$  concentration (approximately 200  $\mu\text{mol l}^{-1}$ ) was observed, indicating no net sulfide production. The produced  $\text{H}_2\text{S}$  was depleted at ca. 400  $\mu\text{m}$  from the surface, while  $\text{O}_2$  penetrated down to ca. 500  $\mu\text{m}$  from the surface, where  $\text{O}_2$  and  $\text{H}_2\text{S}$  coexist. A narrow sulfide oxidation zone (400–650  $\mu\text{m}$  from the surface) was found just above the sulfate reduction zone with a specific  $\text{H}_2\text{S}$  oxidation rate of 16.3  $\text{H}_2\text{S} \mu\text{mol cm}^{-3} \text{ h}^{-1}$ , giving a total  $\text{H}_2\text{S}$  oxidation rate of 0.40  $\mu\text{mol cm}^{-2} \text{ h}^{-1}$ . The specific  $\text{O}_2$  reaction rate was, however, 5.8  $\mu\text{mol cm}^{-3} \text{ h}^{-1}$ , giving a total consumption rate of

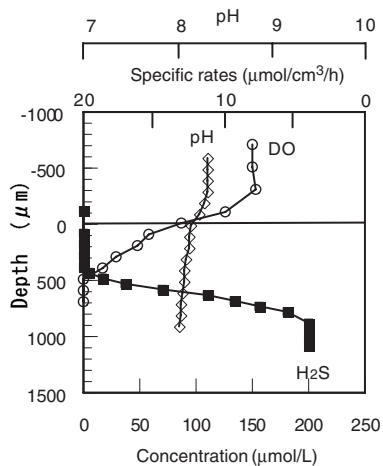


**Figure 1** Concentration profiles of  $O_2$ ,  $NO_3^-$ ,  $H_2S$  and pH in a biofilm incubated in  $156 \mu M O_2$  and  $0 \mu M NO_3^-$ . The biofilm surface is at depth  $0 \mu m$ . Boxes indicate calculated average specific reaction rates ( $R$ )

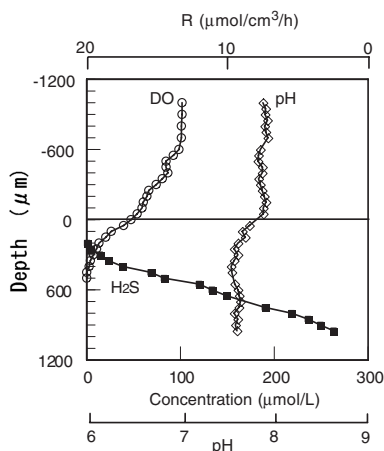


**Figure 2** Concentration profiles of  $O_2$ ,  $NO_3^-$ ,  $H_2S$  and pH in a biofilm incubated in  $100 \mu M O_2$  and  $0 \mu M NO_3^-$ . The biofilm surface is at depth  $0 \mu m$ . Boxes indicate calculated average specific reaction rates ( $R$ )

$0.29 \mu mol cm^{-2} h^{-1}$ . Taking into account that oxidation of 1 mol of  $H_2S$  to  $SO_4^{2-}$  requires 2 mol of  $O_2$ , it was clearly indicated that  $H_2S$  became oxidized with  $O_2$  and other oxidants, probably ferric/ferrous hydrates, and precipitated as  $FeS$  and  $S^0$  in this narrow zone. This speculation was verified by measuring the vertical distribution of reduced sulfur compounds (AVS, CRS, and  $S^0$ ).

A comparable sulfide production rate ( $15.8 H_2S \mu mol cm^{-3} h^{-1}$ ) was observed  $700\text{--}950 \mu m$  below the surface when the bulk DO concentration was slightly reduced to  $100 \mu mol l^{-1}$  (without  $NO_3^-$ ) (Figure 2). The sulfate reduction zone slightly moved toward the biofilm surface, since oxygen penetration depth slightly decreased as compared with Figure 1. However, no free  $H_2S$  was released from the biofilm because of complete internal reoxidation by either chemical or microbial oxidation, or both, within the biofilm at a specific rate of  $12.2 H_2S \mu mol cm^{-3} h^{-1}$ . The sulfide oxidation zone was completely overlapped with the oxygen consumption zone.

The bulk DO concentration was further decreased to  $10 \mu mol l^{-1}$  and the concentration profiles of  $O_2$ ,  $H_2S$  and pH were measured (data not shown). Sulfide production was found even in the uppermost biofilm ( $0\text{--}450 \mu m$ ) and the specific sulfide production rate increased to  $21.1 H_2S \mu mol cm^{-3} h^{-1}$  as well. The sulfide production rate exceeded the sulfide reoxidation capacity because of the low oxygen concentration. Therefore, all possible oxidants including ferric hydroxide ( $FeO(OH)$ ) were saturated with sulfide and consequently, free sulfide was released into the bulk liquid. This evidence was supported by the fact that the biofilm turned black during the measurements (usually taking a few hours). This high level of sulfide production rate was also attributed to the fact that the sulfide production zone moved up to the surface layer where the higher potential sulfate reduction was determined (Okabe *et al.*, 1999). The high sulfate reduction activity was reflected by a decrease in pH in the oxic zone.

The biofilm was incubated with  $100 \mu mol l^{-1}$  of  $NO_3^-$  and  $50 \mu mol l^{-1}$  of DO for at least a few hours and then chemical profiles were measured (Figure 3). Sulfide was produced in  $700\text{--}850 \mu m$  below the biofilm surface with a volumetric rate of  $0.7 \mu mol H_2S cm^{-3} h^{-1}$ . The produced  $H_2S$  diffused up to about  $500 \mu m$  from the surface, whereas  $O_2$  penetrated down to only  $600 \mu m$  from the surface. Thus, the  $H_2S$  profile slightly overlapped with the

O<sub>2</sub> profile but completely overlapped with the NO<sub>3</sub><sup>-</sup> profile over a more than 200 μm-thick zone located about 300 μm from the surface, indicating the occurrence of anaerobic H<sub>2</sub>S oxidation. When NO<sub>3</sub><sup>-</sup> concentration was increased to 280 μmol l<sup>-1</sup>, very low, but detectable, concentrations of H<sub>2</sub>S (below 2 μmol l<sup>-1</sup>) were only detected 1,300–1,450 μm below the biofilm surface with a specific rate of 0.14 μmol H<sub>2</sub>S cm<sup>-3</sup> h<sup>-1</sup> (Figure 4). The sulfide production zone sank in the deeper biofilm and the volumetric sulfide production rate significantly decreased as compared with those without NO<sub>3</sub><sup>-</sup>. The O<sub>2</sub> profile was completely separated from the H<sub>2</sub>S profile, showing the presence of an anaerobic H<sub>2</sub>S oxidation zone. Anaerobic H<sub>2</sub>S oxidation occurred over a 400 μm-thick zone with a specific rate of 0.02 μmol H<sub>2</sub>S cm<sup>-3</sup> h<sup>-1</sup>. Removal of 280 μmol l<sup>-1</sup> nitrate brought about a quick recovery to the previous level of sulfide production activity within 24 hr.

A summary of the effects on DO and NO<sub>3</sub><sup>-</sup> concentrations on sulfide production in the biofilm is listed in Table 1. Total sulfate reduction decreased by addition of NO<sub>3</sub><sup>-</sup> from 0.4 μmol H<sub>2</sub>S cm<sup>-2</sup> h<sup>-1</sup> to 0.002 μmol H<sub>2</sub>S cm<sup>-2</sup> h<sup>-1</sup>. This is because addition of NO<sub>3</sub><sup>-</sup> compressed the sulfate reduction zone and deepened it to the bottom of the biofilm where the specific sulfate reduction rates were lower than at the surface due mainly to the lower SRB

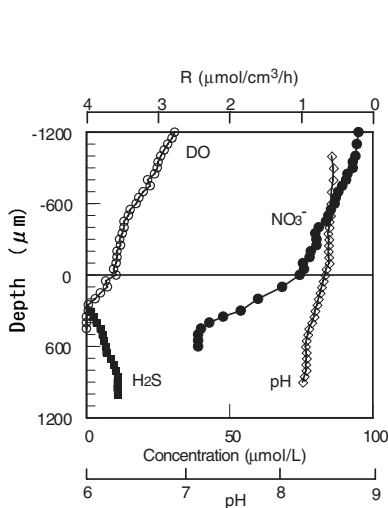


**Figure 3** Concentration profiles of O<sub>2</sub>, NO<sub>3</sub><sup>-</sup>, H<sub>2</sub>S and pH in a biofilm incubated in 50 μmol l<sup>-1</sup> O<sub>2</sub> and 100 μmol l<sup>-1</sup> NO<sub>3</sub><sup>-</sup>. The biofilm surface is at depth 0 μm. Boxes indicate calculated average specific reaction rates (*R*)

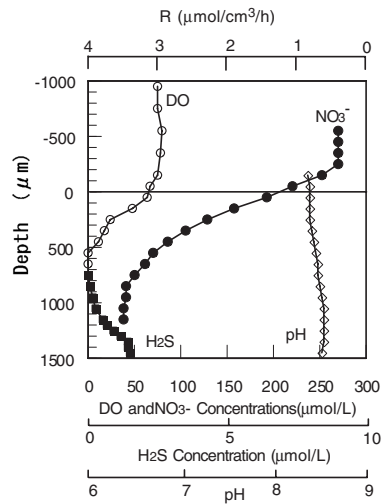


**Figure 4** Concentration profiles of O<sub>2</sub>, NO<sub>3</sub><sup>-</sup>, H<sub>2</sub>S and pH in a biofilm incubated in 70 μmol l<sup>-1</sup> O<sub>2</sub> and 280 μmol l<sup>-1</sup> NO<sub>3</sub><sup>-</sup>. The biofilm surface is at depth 0 μm. Boxes indicate calculated average specific reaction rates (*R*)

**Table 1** Summary of effects of DO and NO<sub>3</sub><sup>-</sup> concentrations on sulfide production rate and sulfide production zone in the biofilm

DO conc. (μmol l <sup>-1</sup> )	NO <sub>3</sub> <sup>-</sup> conc. (μmol l <sup>-1</sup> )	Reaction zone <sup>a)</sup> (μm)	<i>R</i> <sup>b)</sup> (μmol H <sub>2</sub> S cm <sup>-3</sup> h <sup>-1</sup> )	<i>J</i> <sup>c)</sup> (μmol cm <sup>-2</sup> h <sup>-1</sup> )
10	0	0–450	21.1	0.40
100	0	700–950	15.8	0.37
156	0	700–1,000	16.4	0.40
50	100	700–850	0.70	0.006
70	280	1,300–1,450	0.14	0.002

<sup>a)</sup> Presented as depth from the biofilm surface

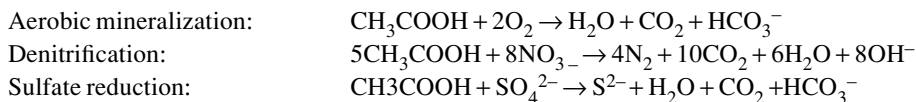
<sup>b)</sup> Average volumetric H<sub>2</sub>S production rate

<sup>c)</sup> Calculated by using Fick's first law from the linear part of the H<sub>2</sub>S profiles between the H<sub>2</sub>S oxidation and the H<sub>2</sub>S production zones

population and possibly a limitation of electron donors resulting from competition with denitrifying bacteria (Okabe *et al.*, 1999). Another possible explanation is either  $\text{NO}_3^-$  directly inhibits sulfate reduction or enhances sulfide oxidation, or both.

#### Acetate mineralization

For estimation of the acetate mineralization budget in the case of Figure 3, it is assumed that acetate is mineralized through three processes such as aerobic mineralization, denitrification and sulfate reduction as expressed by the following stoichiometric equations:



Based on microelectrode measurements, the total acetate utilization rate was estimated to be  $0.007 + 0.013 + 0.006 = 0.027$  [ $\mu\text{mol C cm}^{-2} \text{ h}^{-1}$ ] and the contributions of aerobic mineralization, denitrification and sulfate reduction are 30%, 48% and 22%, respectively. On the basis of the present calculations, a summary of the possible sulfur cycle in an aerobic wastewater biofilm is proposed in Figure 5. The quantitative contribution of organic sulfur compounds to total  $\text{H}_2\text{S}$  production is not clear in this study. Forms of the end products of aerobic and anaerobic  $\text{H}_2\text{S}$  oxidation are dependent on the ratios of  $\text{H}_2\text{S}$  to  $\text{O}_2$  and  $\text{H}_2\text{S}$  to  $\text{NO}_3^-$  in the  $\text{H}_2\text{S}$  oxidation zones. In general, since  $\text{H}_2\text{S}$  production is a rate limiting step, the ratios of  $\text{S}/\text{O}_2$  and  $\text{S}/\text{N}$  are expected to be less than 1.0. Under these conditions, a main product could be  $\text{SO}_4^{2-}$ . Due to accumulation of total S-pool being in the range 3–22% of the total sulfate reduction (data not shown) and reoxidation of the  $\text{H}_2\text{S}$  derived from organic sulfur, the sulfate mass balance remains unchanged.

In the case of Figure 4, the  $\text{NO}_3^-$  concentration was increased about threefold as compared with Figure 3 ( $\text{O}_2 = 70 \mu\text{M}$ ,  $\text{NO}_3^- = 280 \mu\text{M}$ ). All the produced  $\text{H}_2\text{S}$  was oxidized with iron and  $\text{NO}_3^-$  in this biofilm. The same calculation was attempted and the total acetate utilization rate of  $0.105$  [ $\mu\text{mol C cm}^{-2} \text{ h}^{-1}$ ] was found, which is about 4 times higher than that in Figure 3. Aerobic mineralization, denitrification and sulfate reduction accounted for 20%, 78% and 2%, respectively. The contribution of denitrification was increased by a bout 1.6 times and that of sulfate reduction was diminished due to the increase in  $\text{NO}_3^-$  concentration.

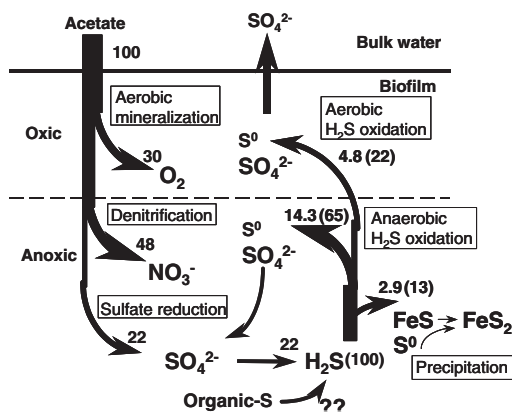


**Figure 5** Summary of the sulfur cycle in a microaerophilic wastewater biofilm (in case of Figure 3).

Numbers are process rates expressed as percentage of the acetate oxidation rate. Process rates in parentheses are expressed as percentage of the sulfate reduction rate

The estimated contribution of SRB to the overall removal of organic matter was comparable with the reported values based on *in vitro* sulfate reducing activities in aerobic wastewater biofilms of a full scale trickling filter and rotating biological contactor showing that SRB accounted for 15–20% of the overall COD removal (Lens *et al.*, 1995). Kuhl and Jorgensen (1992) reported an even higher potential contribution (about 50%) of SRB to the overall removal of organic matter based on sulfide microelectrode measurements.

### Concluding remarks

Microelectrode measurement provides detailed mechanisms for sulfide production occurring within complex sewer biofilms with a typical thickness of only a few millimetres. The results demonstrated the dynamic nature of the sulfur cycle in microaerobic wastewater biofilms. Sequential respiratory processes; O<sub>2</sub> respiration, NO<sub>3</sub><sup>-</sup> respiration, sulfide reoxidation and sulfate reduction were stratified within the biofilms with a thickness of a few millimetres and were highly sensitive to environmental changes. Particularly, an addition of nitrate forced the sulfate reduction zone deeper in the biofilm and significantly reduced *in situ* volumetric sulfate reduction rate as well. The sulfate reduction zone was consequently separated from O<sub>2</sub> and NO<sub>3</sub><sup>-</sup> respiration zones. In addition, the involvement and importance of the iron-sulfur cycle in the overall internal S-cycle was demonstrated based on the measurements of the concentration profiles of reduced sulfur compounds (FeS, FeS<sub>2</sub>, and S<sup>0</sup>) and total-Fe in the biofilm. Reductive and oxidative pathways of sulfur cycle are, however, still very complex, and a further quantitative study is apparently needed to understand sulfide reoxidation in microaerobic biofilms.

### Acknowledgement

This work was supported by the CREST (Core Research for Evolutional Science and Technology), Japan Science and Technology Corporation (JST) and by the Grant-in Aid (No.13650593) for Developmental Scientific Research from the Ministry of Education, Science and Culture of Japan.

### References

- Andrussow, L. (1969). Diffusion, p. 513–727. In *Landolt-Bornstein Zahlenw. Funkt.* Vol. II/5a. Springer, Berlin, Germany.
- Cline, J.D. (1969). Spectrophotometric determination of hydrogen sulfide in natural waters. *Limnol. Oceanogr.*, **14**, 454–458.
- DeBeer, D., Schramm, A., Santeagoes, C.M. and Kuhl, M. (1997). A nitrite microsensor for profiling environmental biofilms. *Appl. Environ. Microbiol.*, **63**, 973–977.
- Fossing, H. and Jorgensen, B.B. (1989). Measurement of bacterial sulfate reduction in sediments: evaluation of a single-step chromium reduction method. *Biogeochem.*, **8**, 205–222.
- Hamilton, W.A. (1985). Sulfate-reducing bacteria and anaerobic corrosion. *Annu. Rev. Microbiol.*, **39**, 195–217.
- Kühl, M. and Jorgensen, B.B. (1992). Microsensor measurements of sulfate reduction and sulfide oxidation in compact microbial communities of aerobic biofilms. *Appl. Environ. Microbiol.*, **58**, 1164–1174.
- Lens, P.N., De Poorter, M.P., Cornenberg, C.C. and Verstraete, W.H. (1995). Sulfate reducing and methane producing bacteria in aerobic wastewater treatment systems. *Wat. Res.*, **29**, 871–880.
- Lorenzen, J., Larsen, L.H., Kjar, T. and Revsbech, N.P. (1998). Biosensor detection of the microscale distribution of nitrate, nitrate assimilation, nitrification, and denitrification in a diatom-inhabited freshwater sediment. *Appl. Environ. Microbiol.*, **64**, 3264–3269.
- Millero, F.J. and Hershey, J.P. (1989). Thermodynamics and kinetics of hydrogen sulfide in natural waters, p. 282–313. In E. S. Saltzman and W. J. Cooper (ed.), *Biogenic Sulfur in the Environment*. American Society for Microbiology, Washington, D. C.
- Mori, T., Koga, M., Hikosaka, Y., Nonaka, T., Mishina, F., Sakai, Y. and Koizumi, J. (1992). Microbial corrosion of concrete sewer pipes, H<sub>2</sub>S production from sediments and determination of corrosion rate. *Water Sci. Tech.*, **23**(7–9), 1275–1282.

- Nielsen, P.H., Lee, W., Lewandowski, Z., Morison, M. and Characklis, W.G. (1993). Corrosion of mild steel in an alternating oxic and anoxic biofilm system. *Biofouling*, **7**, 267–284.
- Norsker, N.H., Nielsen, P.H. and Hvitved-Jacobsen, T. (1995). Influence of oxygen on biofilm growth and potential sulfate reduction in gravity sewer biofilm. *Wat. Sci. Tech.*, **31**(7), 159–167.
- Okabe, S., Itoh, T., Satoh, H. and Watanabe, Y. (1999). Analyses of spatial distributions of sulfate-reducing bacteria and their activity in aerobic wastewater biofilms. *Appl. Environ. Microbiol.*, **65**, 5107–5116.
- Postgate, J.R. (1984). *The Sulphate-reducing Bacteria*, second edition, Cambridge University Press.
- Ramsing, N.B., Kühl, M. and Jorgensen, B.B. (1993). Distribution of sulfate-reducing bacteria, O<sub>2</sub>, and H<sub>2</sub>S in photosynthetic biofilms determined by oligonucleotide probes and microelectrodes. *Appl. Environ. Microbiol.*, **59**, 3840–3849.
- Revsbech, N.P. (1989). An oxygen microelectrode with a guard cathode. *Limnol. Oceanogr.*, **55**, 1907–1910.
- Revsbech, N.P. and Jorgensen, B.B. (1986). Microelectrodes: their use in microbial ecology. *Adv. Microb. Ecol.*, **9**, 293–352.
- Santegoeds, C.M., Ferdelman, T.G., Muyzer, G. and deBeer, D. (1998). Structural and functional dynamics of sulfate-reducing populations in bacterial biofilms. *Appl. Environ. Microbiol.*, **64**, 3731–3739.
- Widdel, F. (1988). Microbiology and ecology of sulfate- and sulfur-reducing bacteria. Chapter 10. pp. 469–585. In: A.J.B. Zehnder (ed.), *Biology of Anaerobic Microorganisms*, A John Wiley & Sons, Inc., New York, USA.